

A new propeller EPI design using short axis readouts

S. Skare¹, R. Newbould¹, D. B. Clayton¹, R. Bammer¹

¹Radiology, Stanford University, Palo Alto, CA, United States

Introduction: EPI suffers from various artifacts such as geometric distortions, Nyquist ghosting, T_2^* blurring, Maxwell effects and eddy currents (especially for DW-EPI). The magnitude of these artifacts is inversely scaled by the speed of k-space traversal along the phase encoding direction (a.k.a. pseudo bandwidth), which is determined by two factors: a) the time between two consecutive echoes in the EPI readout train and b) the phase field-of-view (FOV). For some field inhomogeneity, $\Delta B_0(\mathbf{r})$, the local displacements (in [m]) of the object are given by:

$$d_{pe}(\mathbf{r}) = \frac{\gamma}{2\pi} \Delta B_0(\mathbf{r}) T_{ro} FOV_{pe} = \frac{\gamma}{2\pi} \Delta B_0(\mathbf{r}) \Delta t_{ro} N_{ro} FOV_{pe} \quad [1]$$

where Δt_{ro} and Δt_{pe} are the times between two consecutive sampling points and $T_{ro} = N_{ro} \Delta t_{ro}$ is the readout time for a single echo in the EPI train. Multi-shot EPI reduces the distortions in the p.e. direction since FOV_{pe} , per shot, is reduced. Unfortunately, despite the use of 2D navigators, shot-to-shot phase errors may be induced by motion/diffusion gradients in DW-EPI, leading to ghosting. To cope with these phase errors, the RF refocused PROPELLER sequence (1,4) may be used. This has none of the geometric problems in EPI but is quite SAR intensive, which becomes primarily an issue at higher fields. Inherent navigator capabilities also exist in propeller EPI (2,3). It shares the same k-space trajectory as PROPELLER, with the readout direction along the long axis of the blades (Fig. 1a). We will refer to this propeller EPI implementation as LAP-EPI (Long Axis readout Propeller EPI) in this work for clarity. Still, the real benefit of LAP-EPI is not apparent by scrutinizing Eq. [1]. The distortion level present in LAP-EPI is in fact identical to a standard ssEPI sequence, since readout resolution remains unchanged, but appears as a blurring effect instead of a simple displacement of the object in the phase encoding direction. In this work, the propeller EPI acquisition is redesigned in order to reduce the geometric distortions without relinquishing its advantages. We do this by decreasing the echo spacing by orienting the readout along to the short axis of each blade, hence named SAP-EPI (Short-Axis readout Propeller EPI). The new k-space trajectory SAP-EPI is shown in Fig. 1b. The low resolution in the readout direction governs a short T_{ro} and a high velocity through k-space. Due to ramp times of the gradients, the distortion reduction does not scale linearly with the readout resolution, but e.g. a reduction from 256 to 32 readout points gives about a three-fold reduction of T_{ro} .

Materials and methods: A 1.5T GE Excite system equipped with 50 mT/m gradients was used for the experiments. Our proposed SAP-EPI (Fig. 1b) was compared with LAP-EPI w.r.t. blurring due to Nyquist ghosting and susceptibility. To compare the ghosting levels for the individual blades between LAP-EPI and SAP-EPI, a small cylindrical phantom measuring 10 cm in diameter was used with a FOV of 24×24 cm. The acquired resolutions were 256×32 (LAP-EPI) and 32×256 (SAP-EPI) using 25 blades sweeping from 0 to 180°. Images were also acquired on a volunteer using conventional ssEPI, LAP-EPI and SAP-EPI, with the same parameters and target resolution of 256×256.

Results: In Fig. 2a, LAP-EPI propeller blade for angles 0°, 45°, 90°, 135°, 180° are shown after automated Nyquist ghost correction (separate abstract) and individual regridding. The highest residual ghosts are seen for 45° and 135°, in which the logical readout is driven equally by the physical x and y gradients, which causes maximal shift in the k_{pe} direction (5), which is not correctable by readout phase modulation (ref-correction). These ghosts translate into blurring in the final all-blade image. For the SAP-EPI sequence (Fig. 2b), with shorter N_{ro} , the ghosting in corresponding blades is barely noticeable. A slice just superior to the auditory canals of the volunteer is displayed in Fig. 3, acquired with ssEPI, LAP-EPI and the proposed SAP-EPI. For ssEPI, the well-known signal pile-up is evident, which may obscure important structures. For LAP-EPI, the distortions seen in ssEPI are together with additional Nyquist ghosting (Fig. 2a) translated into blurring. This results in a reduction of the effective resolution about an order of magnitude. With the 32×256 SAP-EPI (Fig. 3c), the image quality is greatly improved compared to Fig. 3a-b. Only with SAP-EPI can the anterior sulci be appreciated.

Discussion & Conclusions: Geometric distortions and ghosting are challenging for EPI in research and clinical practice. In this paper we have presented an improved propeller EPI sequence with redesigned propeller blades using short-axis readouts. While maintaining PROPELLER EPI advantages, our method has markedly less blurring and distortion compared to the earlier propeller EPI method. The advantage over both LAP-EPI and Cartesian EPI becomes more prominent at higher target resolutions, as increased resolution does not result in increased distortion in SAP-EPI.

References: 1) Pipe JG. *Magn Reson Med* 1999;42(5):963-969. 2) Wang FN *et al.* *Magn Reson Med* 2005;54(5):1232-1240. 3) Chuang TC *et al.*; 2004; Kyoto. p 535. 4) Forbes KP *et al.* *J Magn Reson Imaging* 2001;14(3):215-222. 5) Grieve SM *et al.* *Magn Reson Med* 2002;47(2):337-343.

Acknowledgements: This work was supported in part by the NIH (1R01EB002771), the Center of Advanced MR Technology at Stanford (P41RR09784), Lucas Foundation, and Oak Foundation.

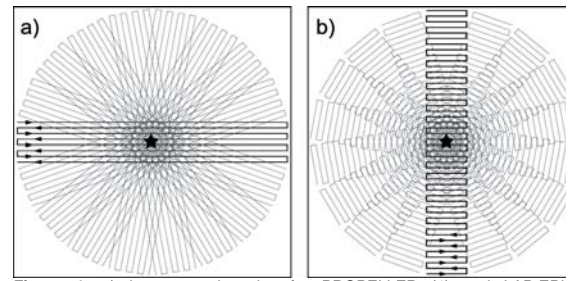


Figure 1. a) k-space trajectories for PROPELLER (1) and LAP-EPI implementations(2,3). b) k-space trajectory for the SAP-EPI sequence proposed in this work. Pentagrams denote the center of k-space.

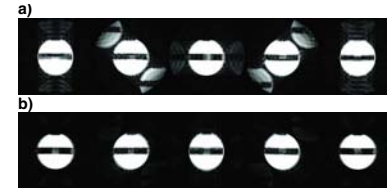


Figure 2. Residual ghosting as a function of blade angles (0°, 45°, 90°, 135°, 180°) for a) 256×32 LAP-EPI and b) 32×256 SAP-EPI. The ghosting is efficiently removed for all angles in b), while significantly residual ghosting is present for oblique blades for LAP-EPI. This ghosting will translate to additional image blurring in the final regridded image.

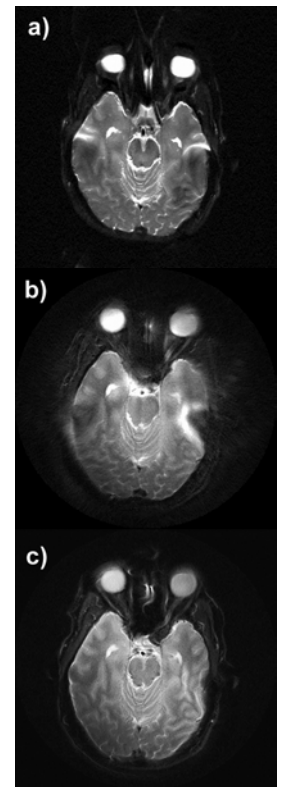


Figure 3. a) 256×256 ssEPI, b) 256×32 LAP-EPI, c) 32×256 SAP-EPI. ssEPI and LAP-EPI are equally sensitive to susceptibility, which appears as unidirectional distortion and blurring, respectively. Residual Nyquist ghosts (Fig. 2) translate to blurring for LAP-EPI. For our SAP-EPI (c), the blurring present in b) and distortions present in a) are considerably reduced.